Pile groups under vertical and inclined eccentric loads: elastoplastic modelling for performance based design

Andrea Franza[a,*], Brian Sheil[b]

[a]*Department of Engineering, Aarhus University, 8000, Aarhus, Denmark.*
[b] *Department of Engineering Science, University of Oxford, OX1 3PJ, Oxford, United Kingdom.*

Abstract

This paper presents a numerical study of 3×3 pile groups embedded in clay under vertical and inclined eccentric loads. Simplified modelling, based on elastic beams embedded in a soil continuum, is used to explore the soil-pile-cap response. This simple model allows rigorous treatment of the 3D foundation geometry and local soil plasticity, demonstrated through validation with advanced finite element analysis. The numerical results reveal that complex roto-translational displacements of the pile group are induced by eccentric or inclined loads, with highly nonlinear relationships when soil plasticity is considered. Interestingly, vertical eccentric loads mobilise the lateral soil resistance at large cap displacements. Thus, while existing t-z type models are shown to be adequate for serviceability predictions, they could provide overly-conservative estimates of the ultimate load capacity. Also, foundation internal forces can exceed allowable bending moments of reinforced concrete piles under multi-directional loads. For performance based design of pile groups under inclined eccentric actions, engineers should estimate the impact of soil yielding on both displacements and rotations of the cap, to satisfy limit state requirements. Dimensionless charts are presented, which describe the reduction in vertical capacity, for a prescribed cap displacement, as a function of load eccentricity and inclination.

Keywords: Piles, displacements, soil/structure interaction, elasticity, eccentric inclined loads

*Corresponding author
Email address: andreafranza@gmail.com (Andrea Franza)

Highlights

- Eccentric and/or inclined loads induce nonlinear roto-translational displacements of pile groups.
- Simplified modelling (beams, elastic half-space, localised yielding) compared with advanced analyses.
- Vertical eccentric loads mobilise the lateral soil resistance at large cap displacements.
- Charts for the reduction in vertical capacity, at prescribed cap displacements, due to load eccentricity and inclination.

1. Introduction

Pile groups are one of the most common foundation solutions for large-scale structures such as high-rise buildings and bridge piers, particularly in areas of weaker soil conditions. Traditional pile design focused on predictions of ultimate pile capacity, with often overly conservative factors of safety to ensure that foundation settlements were negligible. Increasing demand for large-scale structures has resulted in a shift towards more economical serviceability limit state design. This has prompted renewed efforts to achieve more accurate predictions of single pile and pile group settlement through more rigorous treatment of both pile-soil and pile-to-pile interactions.

The response of single piles and pile groups to external vertical loads has been researched extensively over the past several decades. This has involved full-scale field investigations (e.g. O'Neill et al. (1982); Mandolini and Viggiani (1997); Ismael (2001); McCabe and Lehane (2006); Dai et al. (2012)), small-scale laboratory testing (e.g. Lee and Chung (2005); Sales et al. (2017); Patra and Pise (2006)), centrifuge modelling (e.g. Zhang et al. (1998); Lam et al. (2009); Zhou et al. (2007)), theoretical analysis (e.g. Chin et al. (1990); Randolph and Wroth (1978, 1979); Zhang et al. (2010); Sheil and McCabe (2016)) and numerical modelling (e.g. Chow (1986); Basile (1999); Leung et al. (2010a,b); Sheil and McCabe (2014); Rose et al. (2013); Comodromos and Papadopoulou (2012)). In contrast, the potential influence of additional moment/torsional effects, due to vertical and horizontal eccentricities of the applied vertical loads, on axial pile capacity has received significantly less attention (Georgiadis and Sheil, 2020). From model tests in sand, Meyerhof and Ranjan (1973), Meyerhof et al. (1981) and Meyerhof et al. (1983) showed that eccentricities and inclinations of the applied load can have a significant influence on the bearing capacity of piles. In particular, it was observed that pile groups experienced a greater deterioration in capacity compared to equivalent single piles. Similar research has been conducted for pile groups founded in clay (Meyerhof and Yalcin, 1984) and layered soils (Yalcin and Meyerhof, 1991; Meyerhof et al., 1981). More recently, Di Laora et al. (2019) used limit analysis theorems to develop interaction diagrams for bearing capacity prediction of pile groups subjected to vertical eccentric loads. Those authors noted that the most common failure mechanism related to 'cap rotation'. In addition to geotechnical considerations, numerous investigators have also shown that eccentric and inclined loading can lead to structural pile failure due to highly non-uniform load sharing (Borello et al., 2010; Andrawes and Caiza, 2012). However, there remains a distinct lack of research into the role of load eccentricities and inclinations on the foundation displacements, which may be related to limit states.

Advanced three-dimensional numerical modelling is becoming more routine in pile group design and allows for the consideration of complex ground behaviour, geometries, and loading paths. A significant drawback is the requirement for detailed ground information (e.g. extensive elemental testing for the calibration of advanced constitutive models), computational resources and pre- and post-processing time. For this reason, simplified models remain an integral part of preliminary foundation design. As discussed in Sheil et al. (2019), computationally efficient simplified models that incorporate soil plasticity and stiffness degradation at the pile-soil interface, whilst retaining elastic interaction between piles, are capable of providing accurate settlement predictions under purely vertical external loads when compared with advanced numerical models and field data. However, nonlinear simplified models have been mostly exploited to evaluate the pile group response under uni-directional loads, in the vertical (e.g. Zhang et al. (2016)), horizontal (e.g. Ooi et al. (2004)), or torsional (e.g. Chen et al. (2016)) direction, while the investigation of the nonlinear coupled response to multi-directional loads has been mostly limited to linear elasticity, to the Authors' knowledge. There is an unmet need to provide design engineers with robust simplified models and design charts that accurately capture pile-pile interaction effects and nonlinear soil-pile transfer mechanisms.

In this paper, simplified numerical modelling, validated by 3D finite element (FE) analysis, is used to explore soil-pile-cap interaction due to inclined eccentric loads for piles embedded in elastic perfectly-plastic soil (referred to as *elastoplastic* herein), which may be considered a first approximation of ground behaviour. Pile groups with rigid elevated caps are analysed, for which there is no cap-soil interaction. The simplified modelling is undertaken using the in-house program 'COMPILE' which allows rigorous treatment of the 3D geometry of the pile group, the presence of the elevated cap (not in contact with the underlying soil), multi-directional loads, and fully coupled pile-soil-pile interaction. The numerical output informs a rational framework for routine performance based design, in the form of dimensionless charts describing the reduction in the vertical design load as a function of load eccentricity and inclination under serviceability or ultimate cap displacement criteria. Numerical predictions of pile group internal forces are used to evaluate the potential for exceeding the structural capacity of reinforced concrete piles for combined axial-flexural actions, possibly to the point of cross-sectional structural failure. The main aim of this paper is to demonstrate the accuracy of elastoplastic continuum-based models in predicting the fully coupled response of pile groups to vertical and inclined eccentric loads.

2. Investigated scenarios

Two idealised 3×3 pile groups with a rigid elevated cap and embedded in homogeneous undrained clay overlying rigid bedrock are studied. The pile group is subjected to monotonically increasing inclined eccentric forces. Figure 1 illustrates the problem geometry, including pile group configurations and load conditions.

All reinforced concrete piles have a diameter $d = 0.5$ m, embedment length $L = 12.5$ m, and spacing s between the pile centres of either $2.5d$ or $5d$. Pile behaviour is assumed linear elastic with Young's modulus $E_p = 30$ GPa and Poisson's ratio $\nu_p = 0.15$. Fixed connections between the pile heads and pile cap are adopted in the modelling. The clay stratum has a thickness $H = 37.5$ m, undrained shear strength $s_u = 20$ kPa, undrained Young's modulus $E_s = 10$ MPa (to give a typical E_s/s_u ratio of 500), and Poisson's ratio $\nu_s = 0.495$.

In this paper monotonic load paths are applied to the pile group. To study multi-directional actions, an inclined point load of magnitude f is applied to the rigid cap at the location $(e_x, 0, -0.5\,\text{m})$ referred to as the *loading point*, defined by an eccentricity e_x from the cap centre along the x-direction and an inclination angle α_x to the vertical. Boundary conditions considered for the external load include $e_x/d = 0, 1, 2, 3, 5,$ and 10 for $\alpha_x = 0, \pm15°, \pm30°, \pm45°, \pm60°$. All external actions in this paper are defined with respect to the loading point, while the resulting cap displacements were computed at the *master point* located on the central pile coincident with the soil surface level $(0, 0, 0)$.

For the sake of clarity, note that a force f applied at the load point is equivalent to a force vector comprising a vertical force $f_z = \cos(\alpha) \times f$, horizontal force $f_x = f_z \tan(\alpha_x)$ and negative bending moment

$m_y = -e_x \times f_z$. In other words, the pile group is subjected to a bending moment m_y and a horizontal force f_x both proportional to f_z while being scaled by the eccentricity e_x and the inclination angle α_x, respectively.

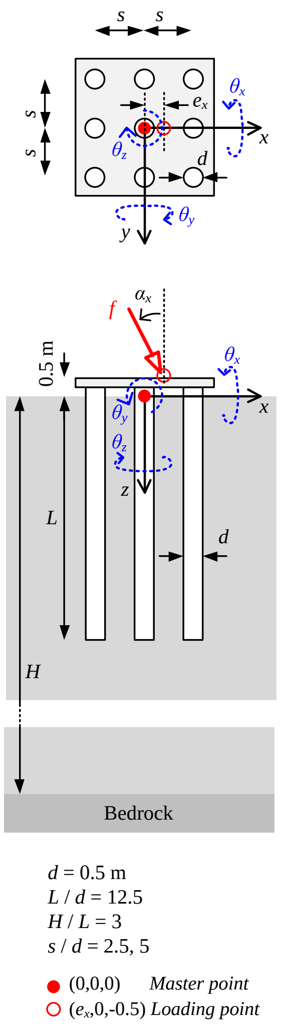

Figure 1: Pile group and load configurations.

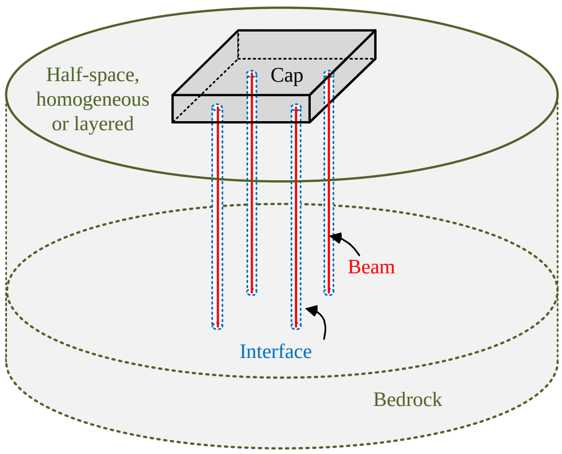

Figure 2: Sketch of the simplified mechanical model.

3. Simplified modelling

The COMPILE model for soil-pile-structure interaction (Franza et al., 2019a,b) consists of beams with nonlinear interfaces embedded in an elastic half-space and is used here for the first time to investigate capped pile groups under multi-directional loads. This simplified mechanical model is shown in Figure 2. It can provide excellent agreement with other half-space based models for vertical and tunnelling-induced actions (Poulos, 1989; Basile, 1999, 2014). However for the considered case of multi-directional external loads, a thorough validation against advanced modelling (introduced in the next section) is necessary. In the following, this simplified approach is briefly described.

The group of vertical piles is modelled as Euler-Bernoulli beam elements while the elevated rigid cap is modelled using a condensed stiffness matrix. For the soil, Chow's assumption that soil stiffness nonlinearities localise near the pile while the far-field soil region remains elastic is adopted (Chow, 1986). In this paper, the local (*near-pile*) pile-soil interaction for each pile is assumed elastic perfectly-plastic to prescribe the ultimate shaft friction, base pressure, and prevent tensile soil resistance at the pile base. On the other hand, the pile-soil-pile interaction along a given pile and between different piles (referred to as *far-pile*) is described using linear elasticity. The elastic soil behaviour, both in the near- and far-pile regions, is described by a linear elastic and isotropic half-space model (referred to as a *continuum*) which can be either homogeneous or layered. The soil flexibility matrix is obtained by the integrated elasticity solutions for the force-displacement relationship within the half-space (Mindlin, 1936; Ai et al., 2002). At the pile-soil interface, plastic sliders are used to limit lateral and shear forces, which are a function of the pile geometry and soil failure stresses. Note that COMPILE can account for reverse loading, hyperbolic soil stiffness degradation, and ground displacements due to external sources; however, these features are not used in this paper.

The finite element method together with an incremental and iterative procedure are used to solve the equilibrium equations (Franza et al., 2019b). Each pile was discretized into 15 finite elements of 0.83 m length, resulting in a total of 864 degrees of freedom (144 nodes with six degrees of freedom each) for the pile foundation system; this reduced mesh size is key to achieving computational efficiency in simplified modelling whilst also preserving prediction accuracy.

The suitability of simplified modelling for preliminary foundation design is further enhanced by the reduced number of rational input parameters. In addition to defining the problem geometry (parameterised in COMPILE), mechanical inputs required by the model are: the Young's modulus and Poisson's ratio of the soil (E_s, ν_s) and piles (E_p, ν_p); the ultimate values of the shaft friction $\tau_{s,f}$ (per unit shaft area) and horizontal shaft pressure $\sigma_{s,f}$ (per unit pile length) along the length of the pile, and the vertical base pressure $\sigma_{b,f}$ (per unit base area).

Any rational methodology may be implemented to estimate the soil ultimate stresses, which is taken as an input in the simplified model. In this paper, the alpha-method is selected to simulate undrained soil failure. Pile shaft friction and base pressure at failure are taken as $\tau_{s,f} = s_u$ and $\sigma_{b,f} = 9s_u$, from which it follows that the ultimate vertical load of a single pile is estimated analytically as 495.2 kN while the ultimate (purely) vertical load of the pile group is $f_{z,u} = 9 \times 495.2\,\mathrm{kN} = 4.46\,\mathrm{MN}$. For the ultimate lateral soil pressure, Broms's (Broms, 1964) distribution is assumed, for which $\sigma_{s,f}$ linearly increases between $2s_u d$ and $9c_u d$ from surface to a depth of $3d$ at which point it becomes constant (Fleming et al., 2009).

4. Advanced models using Plaxis

Advanced numerical models were developed using the FE software package Plaxis 3D 2019. Two sets of analyses were completed wherein the soil was modelled as: (a) a weightless elastic material, and (b) a weightless elastic-plastic Tresca material. The piles were modelled using 'volume elements' conforming to linear elastic behaviour. Interface elements were also introduced at the pile-soil interface with the same properties of the soil. The rotations and displacements of the pile heads were coupled to those of the corresponding elements in the cap. The rigid cap had a plan area of $10d \times 10d$ to allow a wide range of load eccentricities to be explored.

A challenge in modelling bearing capacity problems using FE analysis is the sensitivity of the calculation to the refinement of the mesh, particularly in the vicinity of the piles. Compared with 2D modelling, there is also a more intensive element requirement for 3D modelling to achieve an equivalent satisfactory level of accuracy. This makes for a much more onerous manual mesh development process due to the requirement for numerous mesh iterations and considering that the correct solution is approached from the unsafe side. In addition, the potential for 'volumetric locking' to occur when modelling failure of nearly incompressible material has been well documented (e.g. Monforte et al. (2017); Zhou et al. (2007)). Volumetric locking occurs due to an inability of the FE functions to properly approximate a volume-preserving strain field which can lead to gross underestimates of soil displacements for geotechnical problems. This is problematic as it cannot be overcome by further mesh refinement and is instead alleviated using elements with high-order or reduced integration (Chen et al., 2000; Heisserer et al., 2007).

In light of these issues, the soil and pile were modelled using 10-node tetrahedral elements while the rigid pile cap was modelled using 6-node plate elements. An exemplar pile group mesh is shown in Figure 3 including the size of the adopted computational domain (i.e. distances to external boundaries). A large number of elements was adopted to achieve a high level of accuracy. Lateral boundaries were restricted from movement normal to their respective surface whereas the bottom boundary was fully fixed.

The calculation stages adopted in these analyses are as follows: (1) initialisation of soil stresses; (2) 'wished in place' installation of weightless piles; (3) Installation of the weightless rigid pile cap; (4) application of a prescribed point load on the pile cap with eccentricity e_x and inclination to the vertical of α_x.

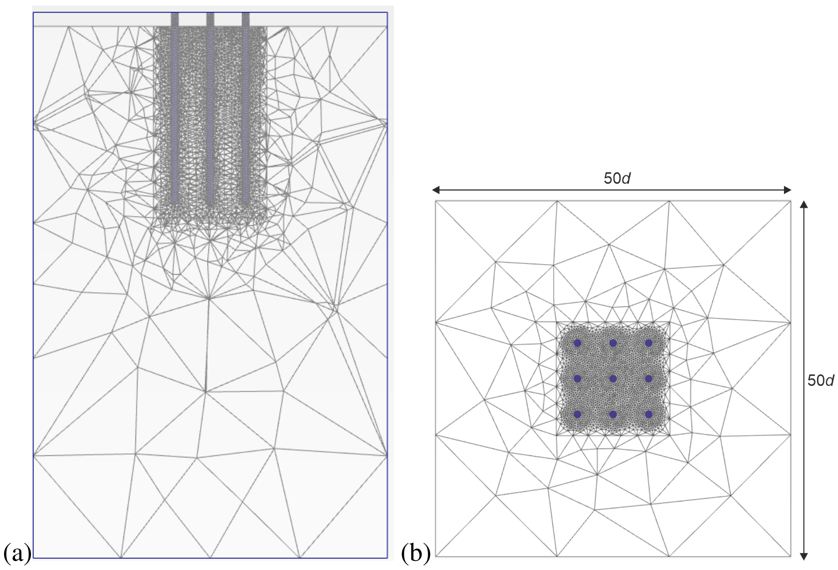

Figure 3: Schematic illustration of an exemplar finite element mesh for a 3×3 pile group (approximately 400k nodes): (a) elevation and (b) plan view.

5. Foundation displacements

In this study, the vertical component of the external force f_z is normalised by the computed group capacity for purely vertical actions ($f_{z,u}$=4.42 MN) to produce a *vertical force factor* $\beta_z = f_z/f_{z,u}$. Furthermore, in performance based design the allowable loads at the serviceability (SLS) and ultimate (ULS) limit states are typically defined using threshold foundation displacements (e.g. Zhang and Chu (2009)). These limits may be applied to the vertical (u_z), horizontal (u_x), or total ($u_{tot} = \sqrt{u_z^2 + u_x^2}$) cap displacement. In this paper, either the vertical u_z or total u_{tot} displacements of the master node corresponding to $2\%d$ and $10\%d$ are used to define the SLS and ULS, respectively. However, any other displacement requirement may be selected by the designer.

The effect of eccentric vertical loads on the roto-translational behaviour of the pile group is first addressed. Figures 4 and 5 display the normalised settlement (u_z/d), horizontal displacement (u_x/d), and rotation (θ_y) of the master point plotted against the vertical force factor β_z, as predicted by both the simplified and advanced models. The results show that while the eccentricity does not influence the initial elastic vertical displacements, it decreases the vertical forces at large settlements u_z/d, in qualitative agreement with classical perfectly-plastic theories (e.g., Di Laora et al. (2019)). Also, the eccentricity has a significant influence on both u_x/d and θ_y over the full load range. Comparing Plaxis and COMPILE predictions in these figures, despite some differences in the initial rotational and horizontal stiffness, particularly for the smaller spacing $s/d = 2.5$, simplified modelling predictions are mostly satisfactory, particularly within the intermediate range of $\beta = 25\%$ and 75%. However, a deviation between settlement predictions is distinguishable for the $e_x = 0$ case in subplots (a) of these figures. This indicates that at $\beta > 75\%$ (a relatively high loading level in practice), soil in between piles may reach a plastic state in the advanced modelling particularly for closely spaced piles (Khatri and Kumar, 2009), making the far-soil elasticity assumption of the simple model not fully applicable. Nevertheless, the simplified modelling predictions show overall good agreement, particularly for the eccentric vertical loads, confirming the suitability of this model for preliminary assessments.

Next, the pile group stiffness is analysed in detail by considering results in Figures 4 and 5. At the (nearly elastic) small load regime a reduction in the pile spacing from $s/d = 5$ to $s/d = 2.5$ influences, as expected, the pile group vertical response by increasing the elastic pile-to-pile interaction and, consequently, the group settlement u_z. Also, an increase in eccentricity causes a reduction in the initial stiffness of u_x/d and θ_y for $s/d = 2.5$ compared to $s/d = 5$, due to the smaller distance of piles from the pivot (master) point. Note that the load eccentricity e_x results in a negative rotation θ_y of the pile cap, associated with a positive horizontal translation of the foundation u_x (see Figure 1 for the reference system). This cap rotation is consistent with the negative bending moment m_y caused by a positive eccentricity e_x. Also, the roto-translational coupling is due to the lateral soil resistance mobilised by the bending of piles, which is in turn caused by the rotational kinematic constraint imposed by the cap at the pile heads. When considering the nonlinearities in the cap displacements, Figures 4 and 5 show that an increase in the eccentricity causes a significant reduction in β_z at the ULS, regardless of the pile spacing. In fact, in the presence of an eccentricity, vertical factor values between $\beta_z = 25$ and 75% lead to a degradation of the group tangent stiffness in all roto-translational directions because of soil yielding; the greater eccentricity value e_x, the lower the value of β_z which triggers the onset of this tangent stiffness degradation (because of the greater mobilisation of the lateral soil resistance with greater load eccentricities, as further discussed later in the text). Finally, it should be considered that, although low eccentricity loads could satisfy equilibrium for β_z close to 100% (e.g. $e_x/d = 2$ in Figures 4b and 5b) thanks to the lateral soil pressure leading to pile head bending moments, this high β_z required settlement levels well beyond $10\%d$.

To provide insights into the contribution of the lateral soil behaviour towards withstanding vertical

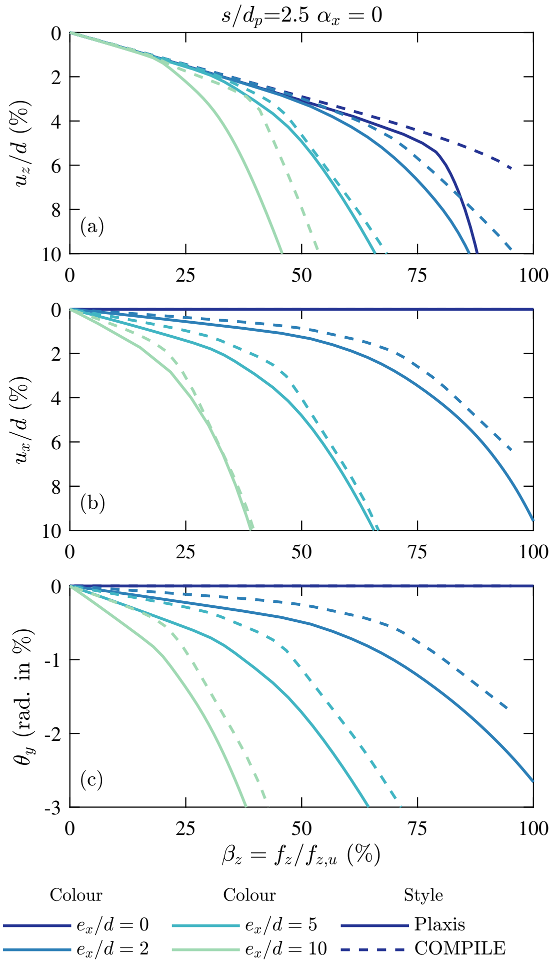

Figure 4: Cap displacements under vertical eccentric loads for a normalised pile spacing $s/d = 2.5$.

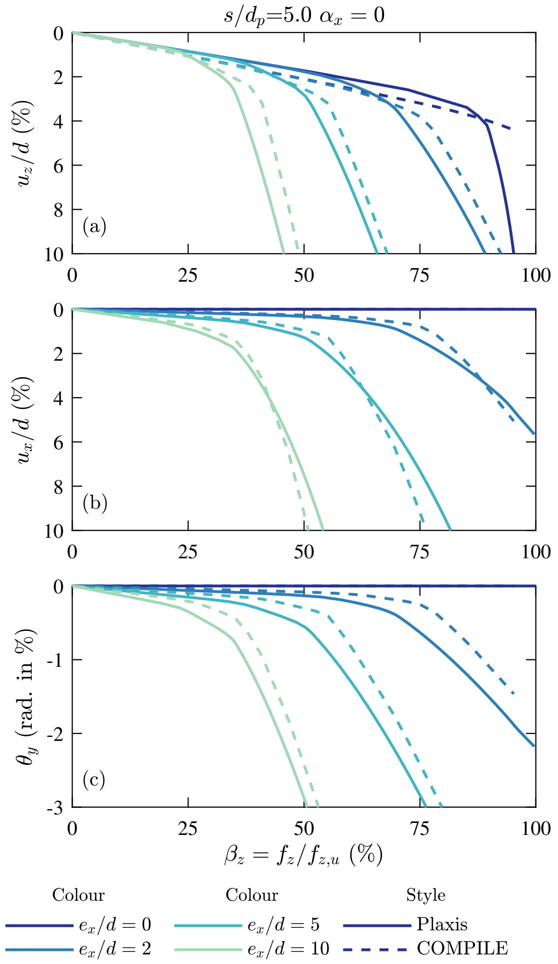

Figure 5: Cap displacements under vertical eccentric loads for a normalised pile spacing $s/d = 5.0$.

eccentric loads, simplified model predictions of cap settlements and rotations are determined using 100% and 0.1% of the horizontal limit stress $\sigma_{x,f}$; the results are compared in Figure 6. Load-displacement curves are identical during the initial loading phase up to a load factor β_z of 20%. However, for the analyses with minimal lateral soil capacity (0.1%$\sigma_{x,f}$), the pile group stiffness starts to degrade quickly, evolving into a brittle mechanism. In contrast, a hardening response is evident at high β_z levels when full lateral capacity is adopted (100% $\sigma_{x,f}$). Thus, Figure 6 gives evidence that the mobilisation of the lateral soil reaction is possibly negligible at the SLS of the soil-foundation system but is a key contributor to the ULS. The results also show that overly conservative estimates of the pile group capacity to vertical loads are possible if this contribution of lateral soil resistance (causing bending moments at the pile heads) is neglected (such as conventional 't-z' approaches assuming piles as vertical springs only).

The load eccentricity is responsible for mobilising the lateral soil strength, in a similar fashion to horizontal loads. Therefore, it is of interest to evaluate how an additional horizontal action f_x (related to α_x) interacts with the bending moment m_y (related to e_x) for eccentric inclined loads. For a pile group with $s/d = 5$, Figures 7 and 8 show load-displacement curves obtained for a positive α_x of 30°and 45°, for which

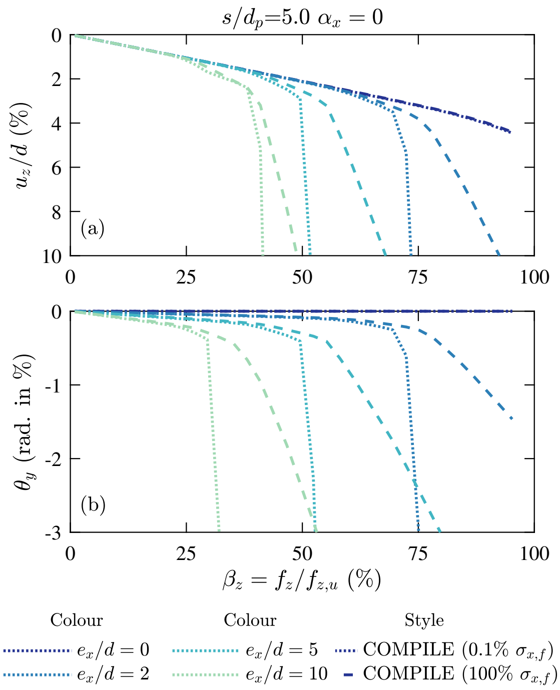

Figure 6: The effect of the lateral limit pressure $\sigma_{x,f}$ on the cap displacements under vertical eccentric loads for $s/d = 5$.

the direction of f_x is towards the positive eccentricity e_x, whereas Figures 9 and 10 display results obtained for the corresponding negative α_x set of $-30°$ and $-45°$.

Model predictions in Figures 7 and 8 obtained for positive α_x values are first discussed. As expected, the presence of the horizontal action f_x amplifies the cap horizontal displacements u_x, which increase in magnitude with α_x. Interestingly, similar to the vertical loads in Figure 5, this horizontal displacement u_x also increases with the eccentricity e_x; however, the influence of the eccentricity on u_x reduces with a decrease in the magnitude of α_x. The inclination angle dominates the cap displacements when the horizontal force is greater than the vertical component. Also, the cap settlement u_z is increased by the presence of a horizontal action f_x in the nonlinear regime when soil yielding leads to a degradation in the foundation system stiffness, though it is negligible at the initial elastic state. Finally, additional negative rotations are induced by positive α_x that further increases the magnitude of θ_y rotations caused by the positive eccentricities. Thus, a horizontal force directed towards the vertical load eccentricity contributes to increasing settlement in the nonlinear regime (i.e. high levels of β_z) while it increases cap horizontal translations and rotations for any value of β_z.

Next, it is also useful to evaluate the complex foundation system response to loads having negative α_x values. Figures 9 and 10 show that negative α_x values (i.e. when the horizontal force action is opposite to the eccentricity of the vertical force) lead to counteracting mechanisms. Negative horizontal displacements and positive rotations are induced by central ($e_x = 0$) loads inclined by negative α_x; however, the introduction of load eccentricity e_x acts to decrease the initial elastic slope of the horizontal displacement curve and reverse the sign of the rotational slope in the elastic regime. Surprisingly, large eccentricities ($e_x = 5$ and $10d$ for $\alpha_x = -30°$; $e_x = 10d$ when $\alpha_x = -45°$) result in tangent stiffness values at the ULS that are opposite to the incremental displacement direction obtained for central ($e_x = 0$) inclined loads (see Figures 9 and 10). Also, note that for negative α_x the variation of β_z corresponding to large settlements (u_z of $6 - 10\%d$) with increasing eccentricity is nonlinear; for instance, at the ULS settlement condition in Figure 9a, vertical forces corresponding to $e_x = 2d$ and $10d$ are greater and lower than the value for central ($e_x = 0$) inclined loads, respectively.

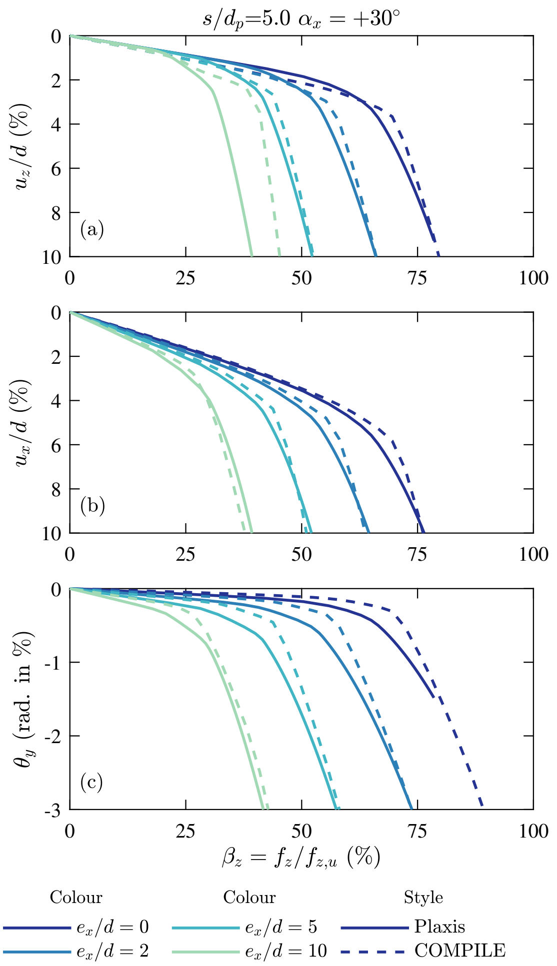

Figure 7: Cap displacements for $s/d = 5.0$ under eccentric loads inclined by $\alpha_x = +30°$.

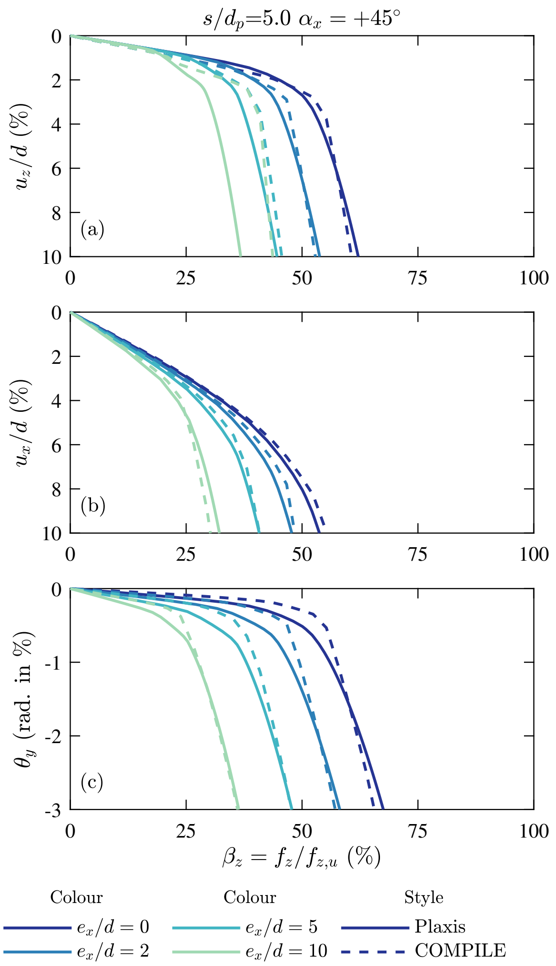

Figure 8: Cap displacements for $s/d = 5.0$ under eccentric loads inclined by $\alpha_x = +45°$.

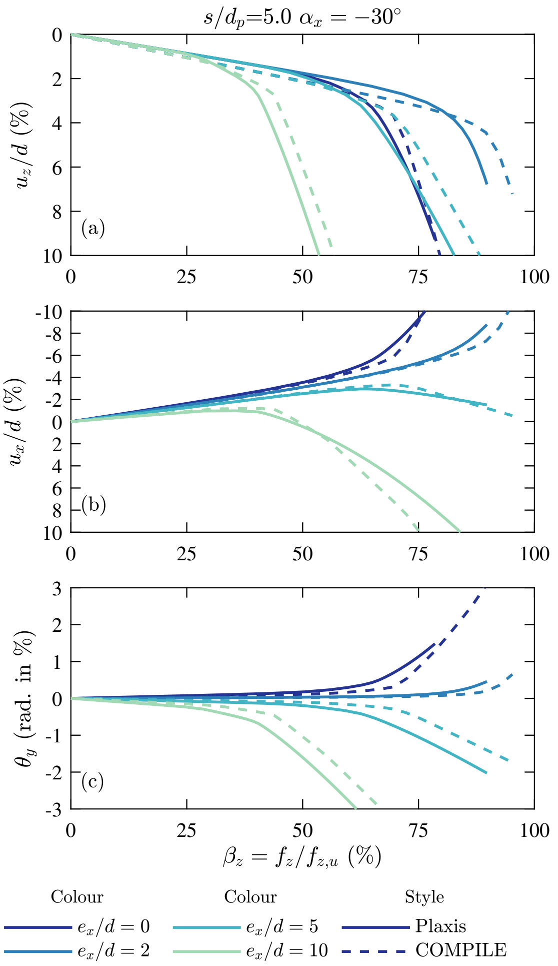

Figure 9: Cap displacements for s/d = 5.0 under eccentric loads inclined by $\alpha_x = -30°$.

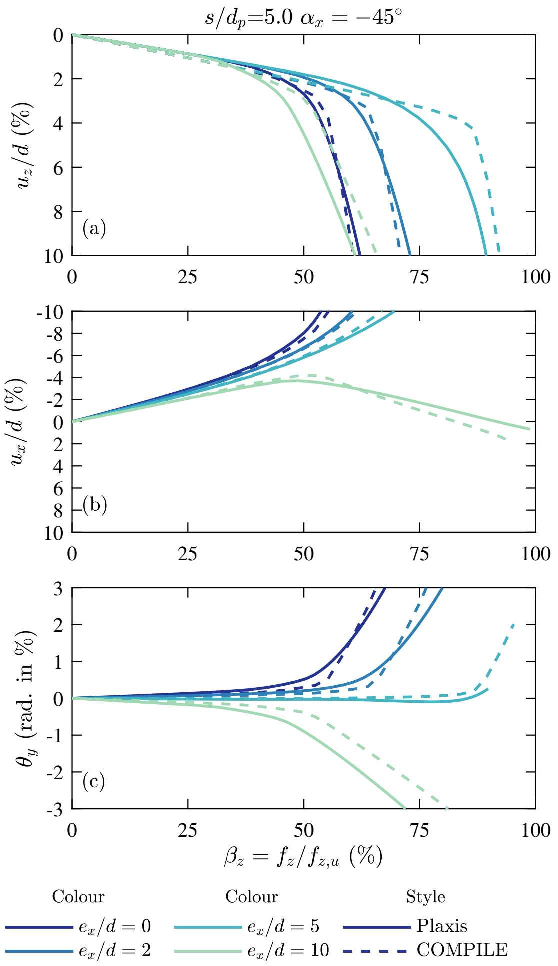

Figure 10: Cap displacements for s/d = 5.0 under eccentric loads inclined by $\alpha_x = -45°$.

Finally, Figures 11 and 12 display the pile displacements (i.e. the foundation deformed shape) using a scale of 50 estimated for $s/d = 2.5$ and 5 from the COMPILE analyses. The figures show both linear elastic (EL) and elastoplastic (EP) predictions of the deformed shape for a fixed load factor $\beta_z = 0.5$ and a variety of boundary conditions; namely, analyses have either no eccentricity $e_x/d = 0$ and $\alpha_x = 30$ or $e_x/d = 5$ and $\alpha_x = -30°, 0, 30°$.

The deformed shapes in these figures give insights into the coupling of horizontal forces and load eccentricity as a result of the cap kinematic constraints, which imposes identical displacements and rotations on all pile heads. For both central horizontal action with no eccentricity (see subplots (a)) and eccentric loads with no horizontal force (see subplots (b)), the external action causes roto-translation of the cap. Interestingly, the external bending moment m_y due to the eccentricity in subplots (b) cause a positive horizontal movement u_x of the cap; this is due to upper-pile bending being counteracted by lower-pile soil resistance thereby restricting lateral movements. Conversely, for the central inclined load in subplots (a), (nearly) the entire pile shafts displace horizontally in the direction of the horizontal force corresponding to a cantilever mechanism. Finally, as displayed by the settlements of both the pile heads and tips, the cap rotation results in differential settlements between piles.

When applying load inclination α_x and eccentricity e_x with identical signs, subplots (c) illustrate that the ultimate lateral pressure of the ground (i.e. lateral soil yielding) is reached in the upper part of piles, as confirmed by the comparisons between the elastic and elastoplastic results. This lateral failure mechanism, inducing cap movements and rotations larger than for the purely elastic case, is due to the fact that positive inclination and positive eccentricity mobilise lateral soil resistance on the identical pile side. However, a counteracting mechanism is displayed by subplots (d) when α_x and e_x have opposite signs, leading to a clear change in the pile curvature along their shafts.

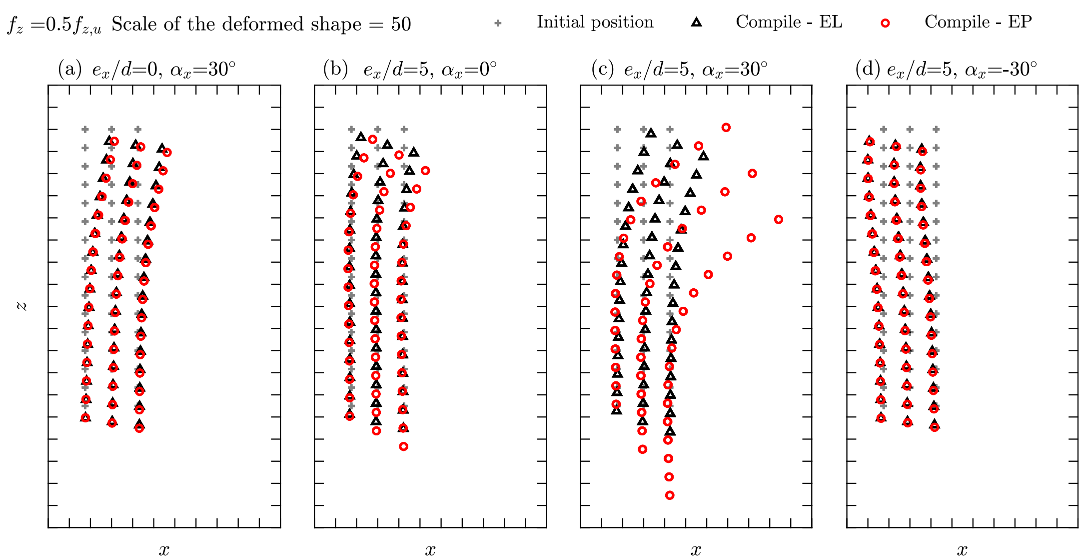

Figure 11: Pile displacements in the x-z plane for a vertical force ratio $\beta_z = 0.5$: (a) $e_x/d = 0$ $\alpha_x = 30°$, (b) $e_x/d = 5$ $\alpha_x = 0$, (c) $e_x/d = 5$ $\alpha_x = 30°$, (d) $e_x/d = 5$ $\alpha_x = -30°$.

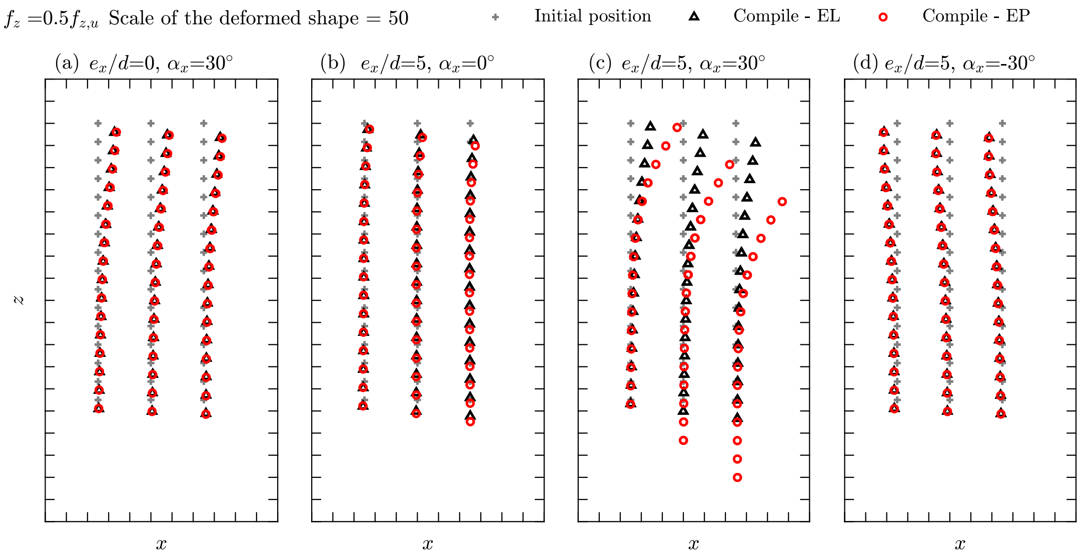

Figure 12: Pile displacements in the x-z plane for a vertical force ratio $\beta_z = 0.5$: (a) $e_x/d = 0$ $\alpha_x = 30°$, (b) $e_x/d = 5$ $\alpha_x = 0$, (c) $e_x/d = 5$ $\alpha_x = 30°$, (d) $e_x/d = 5$ $\alpha_x = -30°$.

6. Interaction charts

For routine preliminary design, it is useful to quantify, in dimensionless terms, the combined effect of the load inclination α_x and the normalised eccentricity e_x/d on the limit state performance of the foundation. To achieve this, Figure 13 shows the isovalue contours (i.e. lines connecting points of equal value) of the vertical load factor β_z at the SLS and ULS (defined as 2% and 10%d thresholds of the cap displacement) for a given α_x and e_x/d. In particular, Figures 13a and b show the limit state factor inferred from limiting the cap settlement u_z, whereas Figures 13c and d display isolines for a criterion set on the total displacement u_{tot}.

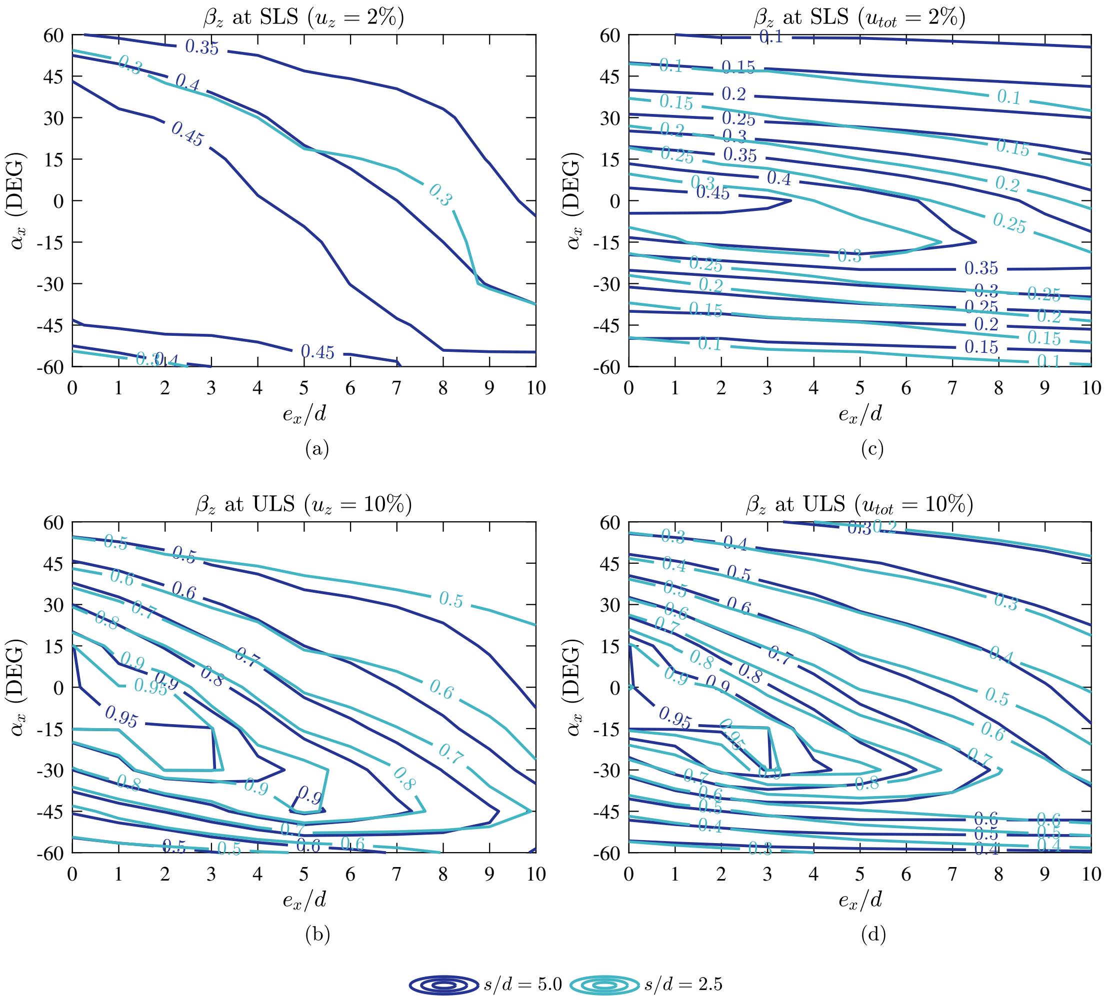

Figure 13: Diagrams of the normalised design vertical load for serviceability and ultimate conditions as a function of load eccentricity and total load inclination: (a) β_z at the SLS defined by $u_z = 2\%$, (b) β_z at the ULS defined by $u_{tot} = 10\%$, (c) β_z at the SLS defined by $u_{tot} = 2\%$, (d) β_z at the ULS defined by $u_z = 10\%$.

First, the influence of the horizontal action is addressed. Interestingly, for SLS and ULS defined with respect to both vertical and total displacements and for a given eccentricity e_x/d, the effect of a positive load inclination $\alpha_x > 0$ on the allowable vertical load is detrimental (i.e. it results in a reduction of the allowable

β_z). On the other hand, the presence of eccentric loads with a negative inclination up to $\alpha_x = -45°$ (the cut-off value varies for each subplot and eccentricity level) may be beneficial, giving slightly greater design β_z than for the corresponding vertical eccentric case ($\alpha_x = 0$, e_x/d). However, beyond this cut-off, increasing the magnitude of the negative inclination causes a steep reduction in the design vertical load.

The eccentricity dominates the pile group performance for small inclinations α_x between $\pm 15°$ while it only induces a slight decline of the allowable β_z when α_x is greater in magnitude than $\pm 45°$. Also, when defining the SLS in terms of the total displacement u_{tot} of the cap, the effect of the eccentricity is marginal. Therefore, for horizontal actions greater than the vertical load (i.e. magnitude of α_x equal to or larger than $\pm 45°$), the eccentricity does not influence the cap displacements for the simplified analyses presented herein.

Finally, it is worth highlighting that the pile group spacing s/d leads to similar qualitative distributions of the isolines and has a minor effect on the allowable β_z. In Figure 13, allowable vertical loads at the SLS tend to be greater for $s/d = 5$ than $s/d = 2.5$, because of pile-pile interaction effects. Furthermore, at ULS, the spacing s/d has minimal effects for negative load inclination ($\alpha_x < 0$) and nonlinear trends for null or positive inclinations ($\alpha_x \geq 0$).

7. Structural pile distress assessment

All analyses presented in this paper considered linear elastic pile behaviour. However, horizontal external forces and eccentric loads lead to foundation flexural and axial deformations associated with pile bending moments and non-uniform distribution of vertical loads (up to tensile forces), as shown in Figures 11 and 12. Therefore, there is potential for pile structural distress and, as a consequence, pile structural nonlinearities that are inhere neglected.

To assess pile integrity, Figure 14 displays cross-sectional $N - M$ charts (bending moment M plotted against axial force N; tensile N are positive while M are reported in absolute terms) to produce *capacity envelopes* that are the ultimate combinations of internal force associated with the cross-section structural failure. Internal forces along the piles are estimated from the COMPILE analyses corresponding to the boundary conditions adopted in Figures 11 and 12 for a vertical factor $\beta_z = 0.5$. Capacity envelopes are inferred from a simple cross-sectional analysis, assuming a stress block ultimate behaviour for concrete, fully yielded steel, and rebar distributed as an equivalent ring (Cosenza et al., 2011). In particular, cross-sectional analyses considered a design concrete strength of $f_{cd} = 14\,\text{MPa}$, design steel strength $f_{yd} = 391\,\text{MPa}$, $d = 0.5\,\text{m}$, cover of $c = 45\,\text{mm}$, and a steel-to-concrete ratio of 1 or 4%. For design, corrective factors of the material properties were proposed by Di Laora et al. (2020).

Figure 14 shows that, at $\beta_z = 0.5$, all analyses would exceed the allowable bending moments if a pile reinforcement ratio of 1% is adopted, while pile integrity is satisfied by a reinforcement ratio of 4% for only specific load conditions. For instance, results obtained under eccentric loads with a vertical action or a positive inclination angle in Figures 14b and c are distributed following a 'U'-shaped pattern in the $N - M$ charts; these cases hold the greatest potential to exceed allowable internal forces when the foundation layout is $s/d = 5$. On the other hand, internal forces for either no eccentricity or a negative inclination angle in Figures 14a and d, which follows 'O'-shaped patterns, are within the capacity envelope for highest reinforcement ratio; also, in all scenarios considered in Figure 14 the spacing $s/d = 5$ leads to slightly higher bending moments than for $s/d = 2.5$. Thus, robust structural design of piles is needed to withstand complex eccentric and inclined loads, with an appropriate selection of the reinforcement in concrete piles.

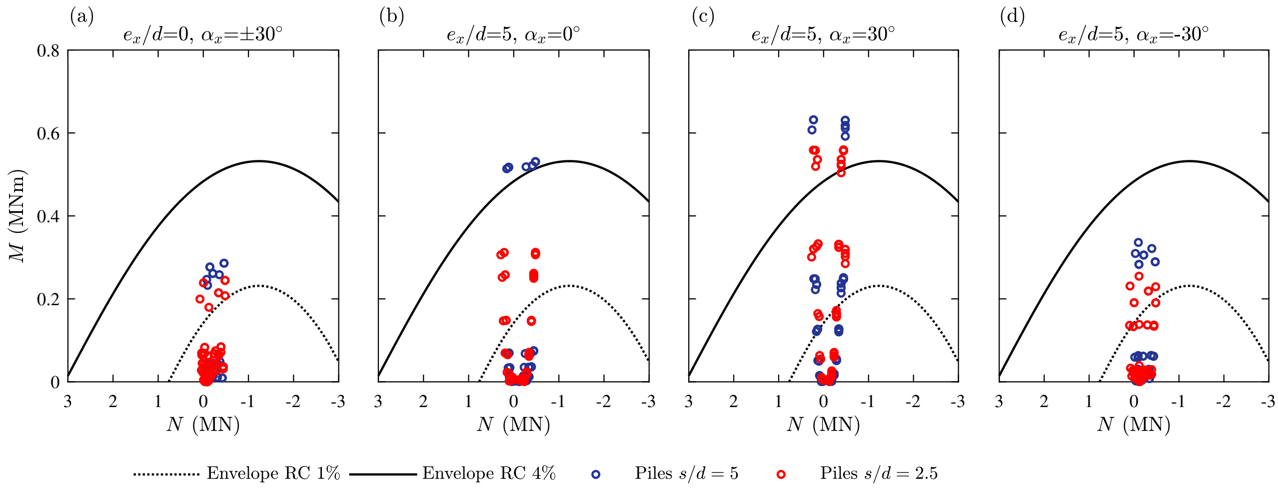

Figure 14: Comparison between pile internal force and allowable envelopes for a vertical force ratio $\beta_z = 0.5$: (a) $e_x/d = 0$ $\alpha_x = \pm 30°$, (b) $e_x/d = 5$ $\alpha_x = 0$, (c) $e_x/d = 5$ $\alpha_x = 30°$, (d) $e_x/d = 5$ $\alpha_x = -30°$.

8. Conclusions

The response of capped pile groups, embedded in uniform undrained clay, subjected to inclined and vertical eccentric loads is studied in this paper. In particular, elastoplastic simplified modelling predictions, consisting of beams with nonlinear interfaces embedded in an elastic half-space, are compared against three-dimensional fully-coupled numerical analyses. The following conclusions are drawn from this work.

- The pile group response to multi-directional loads is affected by complex coupling between the rotation of the cap (and thus pile heads), pile bending and lateral soil behaviour, pile settlements and pile-soil shear. As a consequence, pile groups react to eccentric or inclined loads with a roto-translational mechanism. Therefore, engineers should estimate both displacements and rotations of the cap when vertical or inclined eccentric loads are expected.
- Lateral soil behaviour provides a significant contribution at large displacements (the ultimate limit state) to withstand eccentric applied loads because of the pile capability to resist bending moments at their head when subjected to head rotations imposed by the cap. Neglecting lateral soil resistance (i.e. only considering the vertical soil reaction), frequently done in simplified modelling reported elsewhere in the literature, led to overly conservative ultimate limit state predictions for eccentric vertical loading.
- Pile group performance at the serviceability and ultimate limit states were characterised in terms of settlement or total displacement level of the cap. These displacements are greatly affected by the load inclination and eccentricity, particularly at the ultimate limit state. Results of allowable vertical actions for inclined eccentric external actions are summarised in dimensionless terms, so they can be used as design charts. These charts showed that an increase in load eccentricity induced significant reductions in the allowable vertical load for small load inclinations. In contrast, the eccentricity impact was marginal for horizontal loads greater than the corresponding vertical force. Interestingly, the load inclination always decreased the allowable vertical loads when it produced a horizontal force component in the same direction of the load eccentricity. On the other hand, as long as the horizontal force is smaller than the vertical action, opposite inclinations can improve the vertical foundation behaviour because of the counteracting interaction mechanisms. Qualitatively speaking, the combined effect of the eccentricity and the load inclination did not change with the pile spacing.
- When considering pile groups under multi-directional loads, there is the potential to exceed the structural bending capacity of piles; simplified modelling allows for quick estimates of pile internal forces and, thus, carry out their structural design.
- The versatility of simplified finite element models, with decreased computational requirements and straightforward input definition, is deemed suitable for preliminary design and sensitivity studies of pile group response to complex loading conditions (through predictions of pile settlements and deflections, internal forces and bending moments).

The limitations of this work should be taken into consideration such that the present findings may be extended to practical applications. In this paper monotonic load paths are applied to the pile group. Therefore, engineers should use appropriate judgement if applying the outcomes of this research when load eccentricity and inclination is caused by cyclic or transient external actions. Numerical analyses, both simplified and advanced, were performed assuming wished-in-place pile installation, assuming zero soil weight (which may influence soil failure mechanisms), elastic perfectly-plastic soil with no stiffness degradation, assuming a perfectly rigid pile cap not in contact with the soil, and modelling a linear elastic behaviour of the piles. Future research is warranted to address these aspects and provide an improved description of the problem.

Acknowledgements

This project has received funding from the European Union's Horizon 2020 research and innovation programme under the Marie Sklodowska-Curie grant agreement No 793715. The second author is supported by the Royal Academy of Engineering under the Research Fellowship Scheme.

References

Ai, Z., Yue, Z., Tham, L., Yang, M., 2002. Extended Sneddon and Muki solutions for multilayered elastic materials. Int. J. Eng. Sci. 40, 1453–1483. doi:10.1016/S0020-7225(02)00022-8.

Andrawes, B., Caiza, P., 2012. Bridge Timber Piles Load Rating under Eccentric Loading Conditions. J. Bridg. Eng. 17, 700–710. doi:10.1061/(ASCE)BE.1943-5592.0000300.

Basile, F., 1999. Non-linear analysis of pile groups. Proc. Inst. Civ. Eng. - Geotech. Eng. 137, 105–115. doi:10.1680/gt.1999.370205.

Basile, F., 2014. Effects of tunnelling on pile foundations. Soils Found. 54, 280–295. doi:10.1016/j.sandf.2014.04.004.

Borello, D.J., Andrawes, B., Hajjar, J.F., Olson, S.M., Hansen, J., 2010. Experimental and analytical investigation of bridge timber piles under eccentric loads. Eng. Struct. 32, 2237–2246. doi:10.1016/j.engstruct.2010.03.026.

Broms, B.B., 1964. Lateral resistance of piles in cohesive soils. J. Soil Mech. Found. Div. 90, 27–63.

Chen, J.S., Yoon, S., Wang, H.P., Liu, W.K., 2000. An improved reproducing kernel particle method for nearly incompressible finite elasticity. Comput. Methods Appl. Mech. Eng. 181, 117–145. doi:10.1016/S0045-7825(99)00067-5.

Chen, S., Kong, L., Zhang, L., 2016. Analysis of pile groups subjected to torsional loading. Comput. Geotech. 71, 115–123. doi:10.1016/j.compgeo.2015.09.004.

Chin, J., Chow, Y., Poulos, H., 1990. Numerical analysis of axially loaded vertical piles and pile groups. Comput. Geotech. 9, 273–290. doi:10.1016/0266-352X(90)90042-T.

Chow, Y.K., 1986. Analysis of vertically loaded pile groups. Int. J. Numer. Anal. Methods Geomech. 10, 59–72. doi:10.1002/nag.1610100105.

Comodromos, E., Papadopoulou, M., 2012. Response evaluation of horizontally loaded pile groups in clayey soils. Géotechnique 62, 329–339. doi:10.1680/geot.10.P.045.

Cosenza, E., Galasso, C., Maddaloni, G., 2011. A simplified method for flexural capacity assessment of circular RC cross-sections. Eng. Struct. 33, 942–946. doi:10.1016/j.engstruct.2010.12.015.

Dai, G., Salgado, R., Gong, W., Zhang, Y., 2012. Load tests on full-scale bored pile groups. Can. Geotech. J. 49, 1293–1308. doi:10.1139/t2012-087.

Di Laora, R., Galasso, C., Mylonakis, G., Cosenza, E., 2020. A simple method for N-M interaction diagrams of circular reinforced concrete cross sections. Struct. Concr. 21, 48–55. doi:10.1002/suco.201900139.

Di Laora, R., de Sanctis, L., Aversa, S., 2019. Bearing capacity of pile groups under vertical eccentric load. Acta Geotech. 14, 193–205. doi:10.1007/s11440-018-0646-5.

Fleming, W.G.K., Weltman, A.J., Randolph, M.F., Elson, W.K., 2009. Piling Engineering. 3rd ed., Taylor & Francis.

Franza, A., Marshall, A.M., Jimenez, R., 2019a. Elastic analysis of tunnelling beneath capped pile groups, in: Sigursteinsson, H., Erlingsson, S., Bessason, B. (Eds.), Proc. XVII ECSMGE-2019 Geotech. Eng. Found. Futur., Icelandic Geotechnical Society, Reykjavík, Iceland. doi:10.32075/17ECSMGE-2019-0529.

Franza, A., Marshall, A.M., Jimenez, R., 2019b. Nonlinear soil-pile interaction induced by ground settlements: pile displacements and internal forces. Géotechnique Press doi:10.1680/jgeot.19.P.078.

Georgiadis, K., Sheil, B., 2020. Effect of torsion on the undrained limiting lateral resistance of piles in clay. Géotechnique 70, 700–710. doi:10.1680/jgeot.19.TI.010.

Heisserer, U., Hartmann, S., Düster, A., Yosibash, Z., 2007. On volumetric locking-free behaviour of p-version finite elements under finite deformations. Commun. Numer. Methods Eng. 24, 1019–1032. doi:10.1002/cnm.1008.

Ismael, N.F., 2001. Axial Load Tests on Bored Piles and Pile Groups in Cemented Sands. J. Geotech. Geoenvironmental Eng. 127, 766–773. doi:10.1061/(ASCE)1090-0241(2001)127:9(766).

Khatri, V.N., Kumar, J., 2009. Bearing capacity factor N c under =0 condition for piles in clays. Int. J. Numer. Anal. Methods Geomech. 33, 1203–1225. doi:10.1002/nag.763.

Lam, S.Y., Ng, C.W., Leung, C.F., Chan, S.H., 2009. Centrifuge and numerical modeling of axial load effects on piles in consolidating ground. Can. Geotech. J. 46, 10–24. doi:10.1139/T08-095.

Lee, S.H., Chung, C.K., 2005. An experimental study of the interaction of vertically loaded pile groups in sand. Can. Geotech. J. 42, 1485–1493. doi:10.1139/t05-068.

Leung, Y.F., Klar, A., Soga, K., 2010a. Theoretical Study on Pile Length Optimization of Pile Groups and Piled Rafts. J. Geotech. Geoenvironmental Eng. 136, 319–330. doi:10.1061/(ASCE)GT.1943-5606.0000206.

Leung, Y.F., Soga, K., Lehane, B.M., Klar, a., 2010b. Role of Linear Elasticity in Pile Group Analysis and Load Test Interpretation. J. Geotech. Geoenvironmental Eng. 136, 1686–1694. doi:10.1061/(ASCE)GT.1943-5606.0000392.

Mandolini, A., Viggiani, C., 1997. Settlement of piled foundations. Géotechnique 47, 791–816. doi:10.1680/geot.1997.47.4.791.

McCabe, B.A., Lehane, B.M., 2006. Behavior of Axially Loaded Pile Groups Driven in Clayey Silt. J. Geotech. Geoenvironmental Eng. 132, 401–410. doi:10.1061/(ASCE)1090-0241(2006)132:3(401).

Meyerhof, G.G., Mathur, S.K., Valsangkar, A.J., 1981. The bearing capacity of rigid piles and pile groups under inclined loads in layered sand. Can. Geotech. J. 18, 514–519. doi:10.1139/t81-062.

Meyerhof, G.G., Ranjan, G., 1973. The Bearing Capacity of Rigid Piles Under Inclined Loads in Sand. III: Pile Groups. Can. Geotech. J. 10, 428–438. doi:10.1139/t73-036.

Meyerhof, G.G., Yalcin, A., 1984. Pile capacity for eccentric inclined load in clay. Can. Geotech. J. 21, 389–396. doi:10.1139/t84-043.

Meyerhof, G.G., Yalcin, A.S., Mathur, S.K., 1983. Ultimate Pile Capacity for Eccentric Inclined Load. J. Geotech. Eng. 109, 408–423. doi:10.1061/(ASCE)0733-9410(1983)109:3(408).

Mindlin, R.D., 1936. Force at a Point in the Interior of a Semi-Infinite Solid. J. Appl. Phys. 7, 195–202. doi:10.1063/1.1745385.

Monforte, L., Arroyo, M., Carbonell, J.M., Gens, A., 2017. Numerical simulation of undrained insertion problems in geotechnical engineering with the Particle Finite Element Method (PFEM). Comput. Geotech. 82, 144–156. doi:10.1016/j.compgeo.2016.08.013.

O'Neill, M.W., Hawkins, R.A., Mahar, L.J., 1982. Load Transfer Mechanisms in Piles and Pile Groups. J. Geotech. Eng. Div. 108, 1605–1623.

Ooi, P.S., Chang, B.K., Wang, S., 2004. Simplified Lateral Load Analyses of Fixed-Head Piles and Pile Groups. J. Geotech. Geoenvironmental Eng. 130, 1140–1151. doi:10.1061/(ASCE)1090-0241(2004)130:11(1140).

Patra, N.R., Pise, P.J., 2006. Model Pile Groups Under Oblique Pullout Loads – an Investigation. Geotech. Geol. Eng. 24, 265–282. doi:10.1007/s10706-004-5833-5.

Poulos, H.G., 1989. Pile behaviour - theory and application. Géotechnique 39, 365–415.

Randolph, M.F., Wroth, C.P., 1979. An analysis of the vertical deformation of pile groups. Géotechnique 29, 423–439.

Randolph, M.F., Wroth, P.C., 1978. Analysis of deformation of vertically loaded piles. J. Geotech. Eng. Div. 104, 1465–1488.

Rose, A., Taylor, R., El Naggar, M., 2013. Numerical modelling of perimeter pile groups in clay. Can. Geotech. J. 50, 250–258. doi:10.1139/cgj-2012-0194.

Sales, M.M., Prezzi, M., Salgado, R., Choi, Y.S., Lee, J., 2017. Load-settlement behaviour of model pile groups in sand under vertical load. J. Civ. Eng. Manag. 23, 1148–1163. doi:10.3846/13923730.2017.1396559.

Sheil, B.B., McCabe, B.A., 2014. A finite element–based approach for predictions of rigid pile group stiffness efficiency in clays. Acta Geotech. 9, 469–484. doi:10.1007/s11440-013-0240-9.

Sheil, B.B., McCabe, B.A., 2016. An analytical approach for the prediction of single pile and pile group behaviour in clay. Comput. Geotech. 75, 145–158. doi:10.1016/j.compgeo.2016.02.001.

Sheil, B.B., McCabe, B.A., Comodromos, E.M., Lehane, B.M., 2019. Pile groups under axial loading: an appraisal of simplified non-linear prediction models. Géotechnique 69, 565–579. doi:10.1680/jgeot.17.r.040.

Yalcin, A.S., Meyerhof, G.G., 1991. Bearing capacity of flexible piles under eccentric and inclined loads in layered soil. Can. Geotech. J. 28, 909–917. doi:10.1139/t91-108.

Zhang, L., Chu, L., 2009. Calibration of Methods for Designing Large-Diameter Bored Piles: Serviceability limit state. Soils Found. 49, 897–908. doi:10.3208/sandf.49.897.

Zhang, L., McVay, M., Lai, P., 1998. Centrifuge Testing of Vertically Loaded Battered Pile Groups in Sand. Geotech. Test. J. 21, 281. doi:10.1520/GTJ11367J.

Zhang, Q.q., Liu, S.w., Zhang, S.m., Zhang, J., Wang, K., 2016. Simplified non-linear approaches for response of a single pile and pile groups considering progressive deformation of pile–soil system. Soils Found. 56, 473–484. doi:10.1016/j.sandf.2016.04.013.

Zhang, Q.Q., Zhang, Z.M., He, J.Y., 2010. A simplified approach for settlement analysis of single pile and pile groups considering interaction between identical piles in multilayered soils. Comput. Geotech. 37, 969–976. doi:10.1016/j.compgeo.2010.08.003.

Zhou, X.X., Chow, Y.K., Leung, C.F., 2007. Application of enhanced assumed strain finite element method to predict collapse loads of undrained geotechnical problems. Int. J. Numer. Anal. Methods Geomech. 31, 1033–1043. doi:10.1002/nag.599.